Article

Not peer-reviewed version

Effect of Cetyl Pyridinium Chloride on Corrosion Inhibition Properties of Mild Steel in Acidic Medium

Chandradip Kumar Yadav , Shova Neupane , Benadict Rakesh , Amar Prasad Yadav , Tulasi Prasad Niraula , Ajaya Bhattarai *

Posted Date: 18 April 2024

doi: 10.20944/preprints202404.1187.v1

Keywords: FTIR; FESEM; EDX; inhibitor; mild steel; cetyl pyridinium chloride

 doi:10.20944/preprints202404.1187.v1

Article

Effect of Cetyl Pyridinium Chloride on Corrosion Inhibition Properties of Mild Steel in Acidic Medium

Chandradip Kumar Yadava [1], Shova Neupane [2], Benadict Rakesh [3], Amar Prasad Yadav [1], Tulasi Prasad Niraula [4] and Ajaya Bhattarai [4,*]

[1] Central Department of Chemistry, Tribhuvan University, Kirtipur, Nepal
[2] CIE, DME, University of Southern Denmark, Denmark
[3] CSIR – Institute of Minerals and Materials Technology, Bhubaneswar-751013, India
[4] Department of Chemistry, Mahendra Morang Adarsh Multiple Campus, Tribhuvan University, Biratnagar, Nepal
* Correspondence: ajaya.bhattarai@mmamc.tu.edu.np

Abstract: The corrosion inhibition behavior of cetyl pyridinium chloride (CPC) on mild steel in 0.5 M H2SO4 solution was examined using measurement techniques such as Fourier Transform Infrared Spectroscopy (FTIR), Field Emission Scanning Electron Microscopy (FESEM), and Atomic Force Microscopy (AFM). The studies were carried out within a 25°C temperature range. The surface morphology of the corroded steel samples was investigated using FESEM and AFM. The results show that cetyl pyridinium chloride (CPC), a mild steel corrosion inhibitor, effectively prevents corrosion in 0.5 M H2SO4 and, when present, increases corrosion resistance. CPC has a stronger inhibitory effect on mild steel. The FESEM and AFM images clearly show how surface morphology changes when additives are present. The weight loss results were confirmed by energy dispersive X-ray (EDX) spectroscopy analysis, and a value of 98.54% was obtained from potentiodynamic polarization studies at 0.0077M CPC. CPC acts as an important corrosion inhibitor.

Keywords: FTIR; FESEM; EDX; inhibitor; mild steel; cetyl pyridinium chloride

1. Introduction

Mild steel is widely used in the building, transportation, and maritime industries due to its high mechanical and thermal stability, low cost, and availability. However, mild steel is prone to rust, especially in marine environments [1]. As a result, many methods have been employed to prevent steel from corroding, including electroplating, thermal spraying, micro-arc oxidation, and the application of organic coatings. Organic coatings are the most widely used method of preventing corrosion. Since organic adsorption isolates the steel substrate from corrosive media, it can effectively offer steel long-lasting protection. However, during the curing process, the solvent evaporation of pure organic adsorption might give rise to micropores, which inevitably affects the adsorption's barrier qualities [2]. A fundamental, scholarly, and industrial problem that has received a lot of attention recently is mild steel corrosion. One of the most practical and affordable ways to prevent corrosion on metallic surfaces in very acidic environments is to use inhibitors [3]. In a variety of sectors, pickling steel at temperatures as high as 60°C is a common usage for mineral acids. This technique is effective not only at cleaning industrial equipment but also at acidizing oil wells and eliminating corrosion scales from steel surfaces without destroying the metal [4].

The most potent pickling inhibitors are organic compounds containing heteroatoms, such as oxygen, phosphorus, nitrogen, sulfur, and many linkages or aromatic rings. The amount of loosely bound p-electrons and lone pairs of electrons in these functional groups are important structural elements that affect these compounds' inhibitory effect. These compounds reduce the amount of

 doi:10.20944/preprints202404.1187.v1

active corrosion sites on the metal surface by adsorption, protective layer deposition, or the creation of an insoluble mixture [5].

Unfortunately, the majority of organic compounds used as corrosion inhibitors are dangerous to humans and the environment, thus safer, more environmentally friendly alternatives must be used in their place. Thus, the primary focus of current research trends is the creation of ecologically benign, cost-effective, and nontoxic green chemicals for corrosion inhibition.

Because they are completely soluble in aqueous solutions, biodegradable, nontoxic, and easily manufactured in high purity at a low cost, amino acids are frequently used as corrosion inhibitors[6]. It has been discovered that the sulfur-containing amino acid L-methionine is a potent corrosion inhibitor. Using Tafel polarization measurements, nineteen naturally occurring amino acids—including methionine—were examined for their ability to suppress the corrosion of mild steel in H2SO4 [7].

The current study examined the corrosion inhibition activity of CPC at low concentrations on mild steel in a 0.5 M H_2SO_4 solution. Weight loss, potentiodynamic polarization measures, FTIR, FESEM, and AFM were the characterization techniques used in the present study. Depending on the surfactant concentration, the adsorbed molecules form monolayers, bilayers, or micelles, which block acid from reaching the surface and hence reduce corrosion attacks [8]. The surfactant can boost their effectiveness as inhibitors. Surfactants interact with mild steel surfaces, increasing corrosion resistance [9]. One of the most practical ways to prevent metal from corroding is to utilize organic compounds, such as cetyl pyridinium chloride (CPC), as a corrosion inhibitor. This technique is gaining popularity. Based on available data, organic inhibitors function through adsorption and create a protective coating around the metal. Corrosion can be effectively inhibited by organic compounds like cetyl pyridinium chloride (CPC), which include heteroatoms with high electron density, such as phosphorus, sulfur, nitrogen, and oxygen, or by compounding numerous bonds that act as adsorption centres [10]. Among the inhibitors that work well in acidic solutions are those that contain nitrogen, such as mercapto functional compounds and derivatives of amines like pyridazine, quinoline, and pyridine, as well as pyrazole, pyrazine, acridine, benzimidazole, and triazole. The majority of these compounds have demonstrated mixed-type corrosion inhibition in acidic solutions, protecting mild steel. Benzothiazoles have been employed as corrosion inhibitors for copper and steel in literature reviews [11], although the focus of this paper's studies is on the inhibitory properties of cationic surfactant on mild steel in acidic environments. Surface analytical approaches are needed to characterize corrosion inhibitor films to have a comprehensive understanding of the adsorption mechanism for corrosion inhibitors. According to [12], weight loss and potentiodynamic measurement, FTIR, and Raman spectroscopy have proven to be effective methods for examining corrosion processes and inhibitor performance in various settings.

The capacity of surfactant molecules to assemble at surfaces and in solution is linked to their ability to suppress corrosion. Based on the surfactant inhibitor's micellar characteristics in a given media, its efficacy can be investigated [13].

Depending on the surfactant concentration, the adsorbed molecules form a monolayer, bilayer, or micelle hemimicelles, which lessen corrosion attacks by preventing acid from attacking the surface. To increase other drugs' effectiveness as inhibitors, the surfactant can be employed either by itself or in combination with them [14]. Acids and surfactants are likely to interact to create complex structures that aid in adhesion to the surface and provide increased corrosion resistance [15]. The goal of this investigation is to learn more about how CPC inhibits corrosion on mild steel in a 0.1 M H2SO4 solution. Measurements of weight loss, potentiodynamic polarization, FESEM, EDX, FTIR, Raman spectroscopy, and AFM are among the methods employed.

2. Materials and Methods

2.1. Materials

The mild steel used in corrosion inhibition studies had the following composition (wt%): 0.20 C, 0.53 Mn, 0.036 Si, 0.11 S, 0.098 P, and Fe for the remainder. The examples, which measured 15.92, 13.38, and 1.31 cm, were press-cut from mild steel sheets, machined, and abraded with emery sheets.

 doi:10.20944/preprints202404.1187.v1

This was followed by a rinse with acetone and double distilled water before air drying. Before any experiment, the substrates were produced as directed and used immediately without further storage. The inhibitor CPC (molecular mass: 358 g/mol) was used exactly as received. A stock solution of 0.00192M and 0.0077M CPC was prepared in 0.5 M H2SO4 (AR grade), and the required concentration was obtained through appropriate dilutions. The concentrations of CPC used in the study ranged from low to high. All solutions were prepared using double-distilled water. The experiment was carried out at 25°C, with temperatures maintained using a thermostated water bath. Figure 1 shows the molecular structure of the CPC.

The surface morphology of the steel sample that has corroded both with and without the inhibitors was studied using FTIR (Model no: Bruker company limited, America), FESEM (model: JSM IT800, JEOL Field emission scanning electron microscopy, Made in Japan), EDX (Model no: Elect Super Company EDAX, Made in America) and AFM (model: Jp 02069 JPK Nanowizard, Bruker). The surface morphology of mild steel was studied by looking for surface imperfections, such as pits or obvious abnormalities like cracks, under an optical microscope before any corrosion response began [16][17]. Solely the specimens possessing a smooth, pit-free surface were submerged. The samples were submerged at 25 °C for six hours. Following the test, the specimens underwent a comprehensive cleaning process in double-distilled water, followed by drying and examination with an FTIR, FESEM, and AFM.

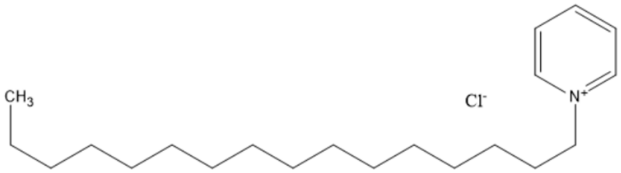

Figure 1. Cetyl pyridinium chloride.

2.2. Weight Loss Measurements

The recently built mild steel specimens were suspended in 50 mL beakers containing 25 mL of the test solution and maintained at 25°C in a thermostated water bath equipped with glass rods and hooks. The weight loss was computed by subtracting the specimens' original weight from their weight at a specific moment in time [8]. Both the uncontrolled solution and the solution containing CPC surfactant mixes were subjected to the measurements. Weight loss experimentation took six hours. The average corrosion rate was determined after the specimens were dipped three times. Less than 5% separated the three identical measurements from one another. The following formula was used to determine the corrosion rates.

$$\text{Corrosion Rate (CR)} = \frac{Weight\ loss\ (W)}{Area\ (A) \times Time(T) \times Density(d)} \times 8.76 \times 10^{4}$$

where W is the weight loss of the MS (g) after immersion time, t (hours), A is the MS's area (cm2), and d is the MS's density (g cm-3).

$$\textbf{Inhibition Efficiency } (\boldsymbol{IE})\ \% = \quad (\boldsymbol{W_o - W_i / W_o})\ \textbf{X 100}$$

where W_o is the MS weight loss in the absence of an inhibitor and W_i is the MS weight loss in the presence of an inhibitor.

$$\text{Inhibition Efficiency (IE) \%} = \text{(Wo -Wi/ Wo) X 100}$$

where Wo is the MS weight loss in the absence of an inhibitor and Wi is the MS weight loss in the presence of an inhibitor.

2.3. Potentiodynamic Polarization Measurements

Three electrode systems were used for potentiodynamic polarization measurements, and each device was Gamry controlled by a PC running AUTOLAB's general-purpose electrochemical system

 doi:10.20944/preprints202404.1187.v1

(GPES) software. The experiments were conducted using. The working electrode is a mild steel sample, the counter electrode is platinum wire, and the reference electrode is a saturated calomel electrode (SCE+ 0.241V) [18].

Potentiodynamic polarization was recorded from -0.3 V to +0.3 V vs. OCP at a scan rate of 0.5 mV/s, examining the potential from cathodic to anodic limits. greater energy than the constant open circuit voltage [4]. All measurements were conducted at room temperature, 25°C. Before starting the measurements, the specimen was submerged in the solution for thirty minutes to create a steady state, as shown by a constant potential. From the measured Icorr values, the IE was calculated using the following relationship [17]:

$$Corrosion\ inihibition\ efficency\ = \frac{I_{Corr} - I^{*}_{Corr}}{I_{Corr}} \times 100\ \%$$

where I*corr = corrosion current when an inhibitor is present, and Icorr = corrosion current when an inhibitor is not present.

3. Results and Discussion

3.1. Weight Loss Measurements

The corrosion behavior of mild steel in 0.5 M H2SO4 with and without varying CPC concentrations was investigated at 25°C using a weight loss approach. Table 1 presents the results of the six-hour immersion. With the temperature at 25°C and the inhibitor concentration, CPC reduces the rate of mild steel corrosion proportionately when compared to a free acid solution [4].

The IE increases with rising CPC concentrations. As inhibitor concentration rises, more CPC molecules are adsorbed on the steel surface at higher concentrations because of the increased IE, which enhances surface coverage and results in the formation of a protective layer. The relatively low IE at lower CPC concentrations may be due to the solubility of adsorbed intermediates generated on the surface as well as the limited surface coverage brought on by the tiny molecular area [19]. At 25°C, individual tests of mild steel corrosion in 0.5 M H2SO4 with and without different CPC concentrations were conducted to examine the impact of CPC on its corrosion-inhibitory behavior. The results are presented in Table 1.

S.N.	Concentration	Corrosion rate (Acm^{-1})	% of Inhibition efficiency
1	0.5 M H_2SO_4	1.20949×10^{-04}	
2	0.00192 M CPC	8.23565×10^{-05}	99.66
3	0.0077 M CPC	6.63607×10^{-07}	99.99

Figure 1. weight loss measurement of mild steel in 0.5 M H2SO4 in the absence of and presence of CPC.

It has been found that IE is more affected by higher surfactant concentrations. The kind and concentration of surfactant molecules determine how they adsorb on surfaces. Although the adsorption of cationic surfactants on like-charged surfaces is less well understood, hydrogen bonding or attractive dispersion forces may play a role, just like in the case of nonionic surfactants. At low surfactant concentrations, the adsorption behavior is typically explained by a simple electrical double-layer model [12]. Catalytic surfactant monomers adsorb as separate ions apart from each other. Tail-tail interactions may cause head groups to face the surface at higher concentrations of adsorbed surfactants. Surfactant monomer head groups form a bilayer on the surface, with one faceting the surface and the other the bulk liquid [20]. The surfactant molecules' adsorption on the

 doi:10.20944/preprints202404.1187.v1

steel surface slows down the corrosion process by lowering the quantity of electrons accessible for reactions. Micelle-like aggregates spontaneously form at far lower concentrations than bulk CMC, and cationic surfactants adsorb to surfaces with opposing charges to form a complete bilayer [21].

3.2. Potentiodynamic Measurement

A potentiodynamic study of a surfactant on mild steel employs electrochemical methods to explore how the presence of the surfactant influences the corrosion tendencies of mild steel. This investigation typically entails immersing mild steel samples in an electrolyte solution containing the surfactant and subjecting them to controlled changes in electrode potential while monitoring resulting currents [22]. Through analyzing parameters such as corrosion potential, corrosion current density, and polarization resistance, researchers gain insights into how the surfactant either inhibits or exacerbates corrosion processes on the mild steel surface. Such studies are crucial for understanding the effectiveness of surfactants in protecting mild steel against corrosion, informing potential industrial applications where mild steel components are exposed to corrosive environments [23].

Using the potentiodynamic polarization methodology, the Tafel polarization approach calculated the corrosion protection potential of CPC as a function of inhibitor concentration and immersion time in a corrosive solution. A thorough description of the results is provided below. The concentration of the inhibitor and length of immersion determine CPC in a corrosive solution [24]. Figure 2 depicts the Tafel polarization behavior of a mild steel electrode immersed in a 0.5M H2SO4 solution blank and exposed to various CPC concentrations [25].

The shape of the anodic and cathodic Tafel slopes provides information on the processes (reactions) taking place on the surface of the mild steel electrode. At the cathodic site, where cathodic currents are produced, electrons released from the breakdown of Fe atoms into Fe2+ ions transform H+ ions into H2 gas, which is the main source of anodic currents [26]. Figure 2 illustrates how the formation of stable corrosive compounds (such as FeCl2) is implied by the falling slope of the anodic branch and comparatively steady current response following around 160 mV of overpotential at the anodic site [27].

Cathodic currents are created at the cathodic site when H+ ions are transformed into H2 gas. The anodic branch slope in Figure 2 decreases following approximately 160 mV of overpotential at the anodic site, signifying the generation of stable corrosive chemicals (such as FeCl2) [28].

The current response then becomes rather steady. The inhibitory efficiency (IE) of CPC at each concentration was determined using Tafel polarization data, and the findings are shown in Table 2. As CPC concentrations rise from 0.00192M to 0.0077M, Figure 2 shows how cathodic and anodic current densities decrease and stable corrosive products (such as FeCl2) form [29].

The anodic current was almost equally reduced by both CPC concentrations, while the cathodic zone shows a stronger tendency [30]. The greatest IE (98.54%) was reached with a CPC concentration of 0.0077 M and an icorr of 0.00025Acm-2. The following formula is used to get IE: Since the effects of the two dosages on anodic sites are almost comparable, the mechanism of concentration-dependent anodic CPC inhibition is most likely at play.

Cl ions may be preferentially adsorbed at anodic sites due to electrostatic contact, covering reactive (anodic) sites, at CPC concentrations of 0.00192M and 0.0077M, respectively. Furthermore, the lower values of a (Table 2) show that the rate of increase in anodic current density is noticeably slower in the presence of both inhibitor dosages than in the absence of them due to the slow rate of Fe dissolution [31].

As concentration increases, anomalous current responses are observed at the cathodic site, where CPC molecules attempt to arrange themselves into different geometrical groups inside the adsorbed layer. Lower CPC concentrations (0.00192 M) appear less effective than higher concentrations, with an IE value of 94.42%. Under the same circumstances, the structure and coatings produce higher IE values in 0.0077 M CPC. At a CPC concentration of 0.0077M, the adsorbed surfactant layer was stable on the mild steel surface.

 doi:10.20944/preprints202404.1187.v1

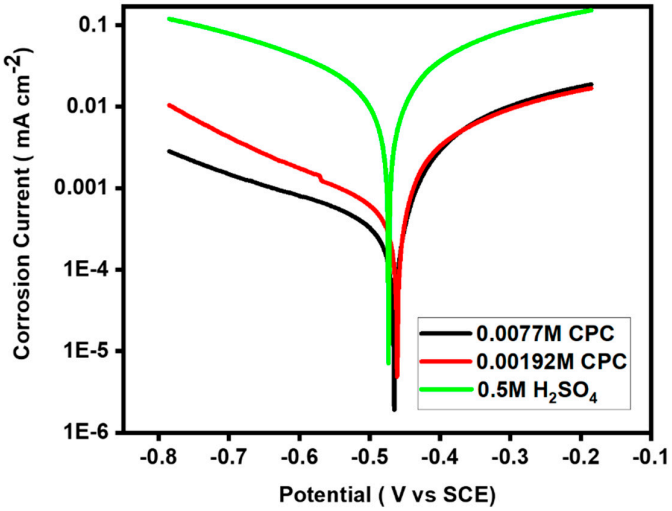

Figure 2. Potentiodynamic curves for mild steel in 0.5 M H2SO4 in the absence of and presence of various concentrations of CPC.

Table 2. Potentiodynamic measurement.

S.N.	Concentration	Corrosion rate (Acm^{-1})	% of Inhibition efficiency
1	0.5 M H_2SO_4	0.01721	
2	0.00192 M CPC	0.00096	99.66
3	0.0077 M CPC	0.00025	99.99

The discovered differences in Ecorr and Icorr between samples shed light on the adsorption's corrosion processes. The evolution of Ecorr values in surfactant-containing samples points to a significant reliance on CPC levels in the CPC-Fe layer. The best balance in this composition of the sample is shown by sample CPC's peak performance, which shows the highest positive Ecorr and the lowest icorr. Additionally, it is shown that samples with higher CPC concentrations have the best corrosion inhibition capabilities.

The sample with the lowest corrosion inhibition characteristics is the one with a lower concentration of CPC. There appears to be a correlation between the molecule's adsorption on mild steel and the thickness of the surfactant layer; samples with lower surfactant concentrations have thinner mild steel layers. It correlates with the strongest corrosion inhibition qualities at greater surfactant concentrations[32].

3.3. Fourier Transform Infrared Spectroscopy (FTIR) of Analysis of CPC

Fourier Transform Infrared Spectroscopy (FTIR) is a technique for determining the functional groups in a sample by analyzing infrared light absorption. It has to do with cetylpyridinium chloride (CPC) precipitation, and the infrared spectra of the precipitate are typically used to identify the functional groups[33]. Moreover, using Fourier Transform Infrared Spectroscopy (FTIR) technology, the Functional Group Identification technique assessed CPC adsorption as a function of inhibitor concentration and immersion time in corrosive solutions [34].

 doi:10.20944/preprints202404.1187.v1

A thorough description of the results is provided below. Figure 3 illustrates the adsorption behavior of a mild steel electrode immersed in a 0.5 M H2SO4 solution blank and exposed to two CPC concentrations. The mild steel functional group provides information on the adsorption process occurring on the surface of the electrode. Figure 3(b) shows the functional group of the CPC molecule. Figures 3(a) and 3(c), respectively, depict the mild steel functional groups before and following immersion in a CPC solution. When CPC molecules come into contact with mild steel, adsorption takes place [35].

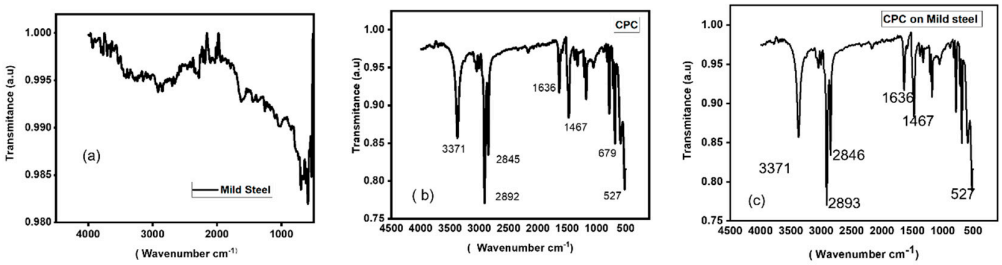

Figure 3. Fourier Transform Infrared Spectroscopy (FTIR) of Mild steel.

Functional Groups in CPC: Quaternary ammonium groups (which have a positive charge on nitrogen atoms) and aromatic rings are two of the functional groups found in cetylpyridinium chloride. Additional functional groups from the interacting chemicals may be present in the precipitate [36]. Aromatic: Usually observed between 1342 and 1266 cm-1 (C-N stretching). Aromatic: Usually detectable between 1690 and 1640 cm-1 (C=N stretching). It is common to detect aliphatic C-H stretching in the range of 3000-2500 cm-1. It is common to see aromatic C-H stretching in the range of 2000-1650 cm-1. The C-H stretching vibrations of the alkyl chain are observable in the 2800-3000 cm-1 range. Figures 3(a), (b), and (c) show the mild steel's adsorbed layer of CPC. This explains why mild steel submerged in CPC solution corrodes at a low pace, which is further corroborated by electrochemical tests.

3.4. Emission Scanning Electron Microscopy (FESEM) study

FESEM analysis was used to examine the morphology of mild steel specimens before and following corrosion (Figure 4), with and without inhibitors. Figure 4(a, b) shows the presence and absence of CPC in an acid solution containing 0.05 M H2SO4[37].

The surfaces of the polished steel samples were uniformly smooth. On mild steel surfaces, however, 0.05 M H2SO4 has a detrimental effect that leads to significant corrosion after 6 hours (Figure 4(a)). The mild steel surface corrodes far less in the presence of inhibitors (CPC) than it does in the blank solution, as seen in Figure 4(b) [38].

It is thought that the inhibitor molecules form an adsorbed layer on the mild steel surface, shielding it from the corrosive species in the solution. Electrochemical tests reveal that the adsorbed CPC layer acts as a barrier between the mild steel surface and the corrosive environment, resulting in a very slow rate of corrosion [39].

 doi:10.20944/preprints202404.1187.v1

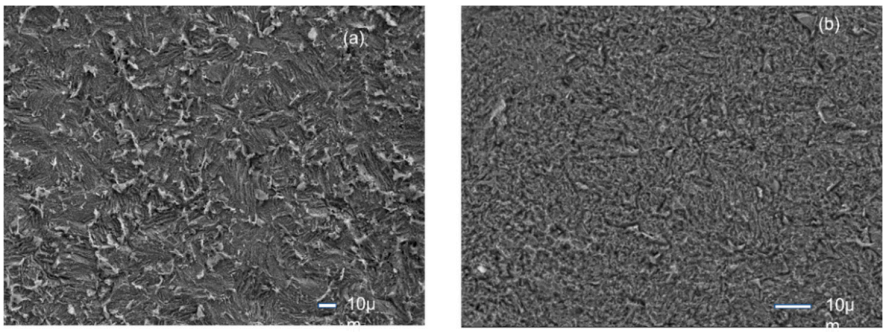

Figure 4. FESEM photomicrograph of the surface of mild steel after immersion in 0.5 M H2SO4, CPC inhibited 0.5 M H2SO4 solution for 6 h at 25 °C.

3.5. X-ray Energy Dispersive Spectroscopy (EDX)

An examination of mild steel Energy dispersive X-ray (EDX) analysis and compositional analysis using electron microscopy are the same. Cetyl pyridinium chloride's effects on mild steel were investigated using energy-dispersive X-ray analysis [37].

The components that are present and distributed on the surface of mild steel both before and after Cetyl Pyridinium Chloride treatment are depicted in Figure 5. The surface composition was determined by EDX analysis, which indicated the presence of mild steel constituents and cetyl pyridinium chloride adsorbed on the mild steel (Figure 5(b)) [40].

According to this investigation, corrosion products were not formed on the mild steel surface after cetyl pyridinium chloride treatment [40]. This illustrates the inhibitory effect of cetyl pyridinium chloride, which forms a layer of protection against corrosion on the mild steel surface. FESEM studies, which demonstrate that the degree of corrosion attack on mild steel reduces as the inhibitor ratio increases, corroborate this conclusion. The EDX experiment additionally demonstrated the physical and spontaneous adsorption of cetyl pyridinium chloride on the mild steel surface.

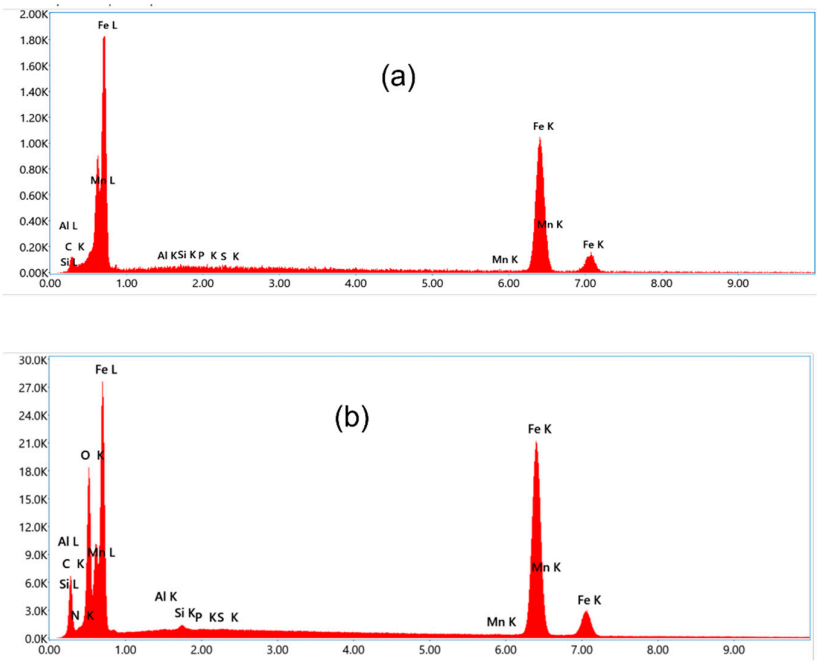

Figure 5. EDX data of mild steel after immersion in 0.5 M H2SO4, CPC inhibited 0.5M H2SO4 solution for 6 h at 25 °C.

 doi:10.20944/preprints202404.1187.v1

3.6. Atomic Force Microscopy (AFM) Study

Studies of mild steel's surface using atomic force microscopy (AFM) in an acidic solution:

The morphological alterations on the mild steel surface, both with and without inhibitors, were also examined using AFM. Figure 6 shows AFM images of mild steel that has been immersed in acid, and different concentrations of surfactant solution [39]. Figure 6a shows pictures of 0.05M H2SO4 acid solution, Figure 6b shows the mild steel in the CPC solution, and Figure 6c shows the 3D picture of mild steel in the CPC solution. Even with the occasional imperfection on the mild steel surface, polished steel retains its homogeneity and smoothness as compared to steel treated with 0.5M H2SO4.

Conversely, inhibitors significantly lessen surface roughness and strengthen the mild steel surface's defence against SO4-2 ion attack (Figure 6(b)), which results in fewer crest peaks and shallow valleys [41]. The surface roughness of the steel coupons can also be computed using the height profiles obtained from AFM analysis (Figure 6(c)). The root mean square (RMS) roughness of the polished steel coupons is displayed [42].

However, after six hours of exposure to 0.5 M H2SO4, the surface has significantly deteriorated and is now displaying RMS roughness. The presence of CPC causes the RMS to drop to 108 nm, indicating the efficacy of the inhibitors.

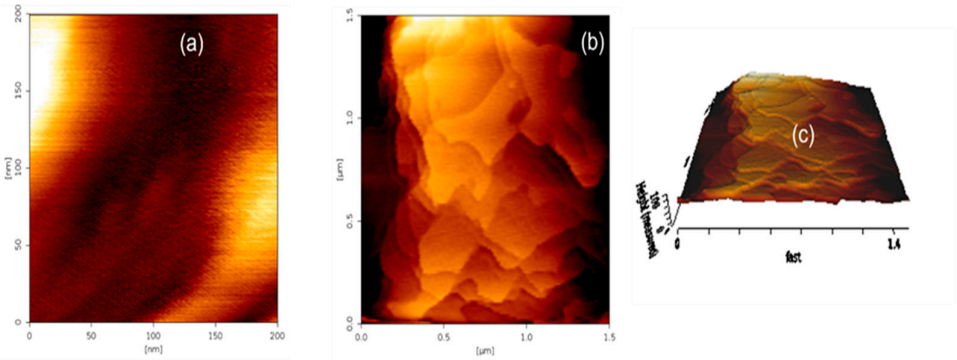

Figure 6. AFM photograph of the surface of mild steel after immersion in 0.5 M H2SO4, CPC inhibited 0.5 M H2SO4 solution for 6 h at 25 °C**.**

The morphologies of mild steel specimens with and without CPC after immersion in 0.5M H2SO4 solutions are shown in Figure 6. Because of the corrosion attack, the surface showed a very uneven topography when the inhibitor was absent (Figure 6). The average roughness of mild steel in 0.5M H2SO4 solution without inhibitor was found to be 46 nm using atomic force microscopy (Figure 6(a)) [39]. A protective inhibitor layer formed on the mild steel surface when CPC was present, reducing corrosion damage and producing a smoother surface with a Ra value of 108 nm (Figs. b and c). Without an inhibitor, it is clear that the mild steel surface was extensively corroded with regions of uniform corrosion (Figure 6 a). Inhibitors, on the other hand, caused the specimen surface to become smoother (Figure 6 (b, c). This is because inhibitor molecules demonstrate a consistently good inhibitory effect by binding with the reaction sites on the mild steel surface, hence limiting the amount of interaction between the mild steel and the aggressive medium.

3.7. Surface Morphological Studies

To find out if the inhibitor adsorption produced a protective layer that prevented corrosion, surface photos of the mild steel specimens were taken using an AFM and a FESEM. Other than polishing scratches, the material's surface appeared to be devoid of apparent defects, pits, and cracks according to the results of the FESEM inspections performed on it before it was submerged in the solutions. [5]. The 0.5 M H2SO4 concentration has no restrictions, which results in a rough and damaged surface.

The addition of inhibitor CPC significantly reduces surface heterogeneity. Figure 4 displays a typical FESEM photomicrograph of the mild steel surface following immersion in a 0.5 mm H2SO4

 doi:10.20944/preprints202404.1187.v1

solution that CPC had occluded [43]. The AFM results of steel specimens produced at 25 °C in the range of and in uncontrolled and inhibited acid solutions, respectively, provide additional support for the FESEM results. The specimen's rough surface and the steel's quick degradation in an uncontrolled acid solution are both visible in the AFM image. The steel surface corrodes less and is noticeably smoother after being coated with CPC [44]. The adsorbed inhibitor creates a more rounded and visually pleasing protective layer. Because some metal areas are not fully covered, they are susceptible to acid attack due to the thin inhibitor coating.

3.8. Interaction of Surfactant, acid, and water with Mild Steel

3.8.1. Surfactant -Acidic Water Interaction

Surfactants are molecules that possess both hydrophilic (water-attracting) and hydrophobic (water-repelling) regions within their structure. the interaction between surfactants and acidic water is complex and can involve various molecular processes such as ionization, hydrophobic interaction, and changes in surface tension and solubility. The specific behavior observed will depend on the properties of the surfactant and the characteristics of the acidic water[45].

When surfactants are introduced into acidic water, several interactions can occur depending on the specific properties of the surfactant and the acidity of the water.

Ionization: In acidic water, the surfactant molecules may undergo ionization. This process involves the dissociation of the surfactant molecule into ions, usually a negatively charged hydrophilic headgroup and a hydrophobic tail. The degree of ionization can vary depending on the pH of the water and the pKa (acid dissociation constant) of the surfactant, which is shown in Figure 7a.

Hydrophobic Interaction: The hydrophobic tails of the surfactant molecules tend to aggregate or associate with each other to minimize contact with water molecules. This can lead to the formation of micelles or other self-assembled structures, where the hydrophobic tails are shielded from the surrounding water molecules, which is shown in Figure 7c [46].

Effect on Surface Tension: Surfactants are known for their ability to reduce surface tension in water. In acidic conditions, the degree of surface tension reduction may vary depending on the specific surfactant and its interaction with the acidic environment. Some surfactants may exhibit enhanced surface activity in acidic water due to changes in their molecular conformation or ionization state.

Solubility: The solubility of surfactants in acidic water can be influenced by factors such as pH, temperature, and the chemical structure of the surfactant molecule. In some cases, the solubility of surfactants may decrease under acidic conditions, leading to phase separation or precipitation of the surfactant from the water [47]. Mild steel was immersed in a surfactant solution then one layer of surfactant was adsorbed on the mild steel surface shown in Figure 7b.i.e there is the origin of the formation of a double layer. These layers help to block the corrosion process of the mild steel.

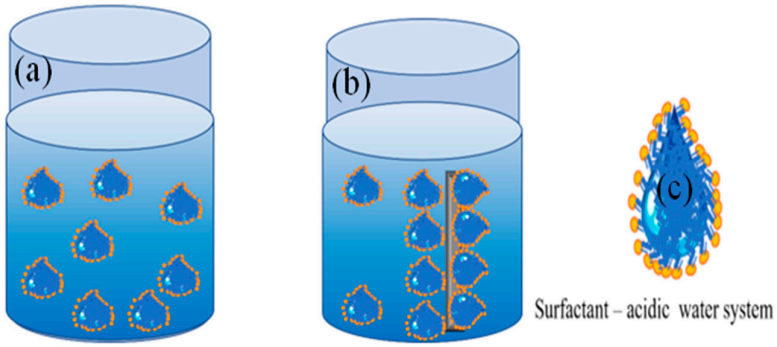

Figure 7. a): surfactant acidic water interaction. b) Micelle of surfactant attached to mild steel. c) structure of aggregation of the surfactant molecule.

 doi:10.20944/preprints202404.1187.v1

3.8.2. Mild Steel - Surfactant -Acidic Water Interaction

When mild steel comes into contact with acidic water in the presence of surfactants, several interactions can occur, which may impact the steel's surface properties and its overall corrosion behavior. the interaction between mild steel, surfactants, and acidic water is multifaceted and can involve corrosion inhibition, surface cleaning, micelle formation, pH buffering, and surface modification processes [48]. The specific impact on corrosion behavior will depend on factors such as the type of surfactant Figure 8c, its concentration, the acidity of the water Figure 8b, and the characteristics of the steel surface Figure 8a.

Corrosion Inhibition: Surfactants act as corrosion inhibitors by forming a protective layer double layer on the surface of the mild steel. In acidic water, where corrosion rates tend to be higher due to increased hydrogen ion concentration, surfactants may adsorb onto the steel surface and hinder the access of corrosive species such as oxygen and ions to the metal surface, thereby reducing the corrosion rate, which is shown in figure 8c. This is clearly shown in the micelle of surfactant attached to the mild steel surface.[49].

Micelle Formation: Surfactants can form micelles in aqueous solutions, where the hydrophobic tails aggregate together while the hydrophilic heads face outward towards the surrounding water. In acidic water, micelle formation may be influenced by factors such as pH and surfactant concentration. [50]. the presence of micelles can affect the adsorption behavior of surfactants onto the steel surface and may influence corrosion inhibition properties [51].

pH Buffering: Some surfactants may exhibit pH buffering properties, which can help stabilize the pH of the acidic water. Fluctuations in pH can influence the corrosion behavior of mild steel, so maintaining a relatively stable pH environment through the addition of surfactants may help mitigate corrosion.

Surface Modification: Surfactants may interact with the surface of mild steel through adsorption processes, leading to modifications in surface properties such as surface charge, wettability, and surface energy. These surface modifications can affect the corrosion resistance of the steel by altering its interaction with corrosive species present in the acidic water [52].

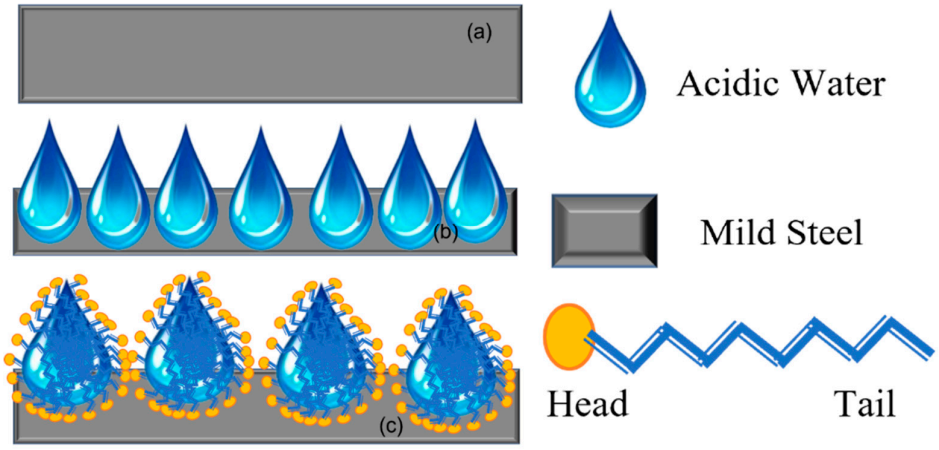

Figure 8. a): Polished mild steel. b) Acidic water on mild steel. c) Surfactant Mild steel, and Acidic water**.**

3.8.3. Mechanism of CPC – Mild Steel

The protonated pyridinium group atom in the molecule is the mechanism underlying the increased adsorption of CPC in acidic liquids. Interaction between the CPC's pyridinium functional group and the corroding steel surface is conceivable shown in Figures 9b and 9c. Protonated pyridinium's functional group is adsorbed at anodic sites to prevent iron dissolution and at cathodic sites to halt the hydrogen evolution reaction Figure 9a. [15].

 doi:10.20944/preprints202404.1187.v1

This implies that the anodic and cathodic partial responses are regulated by the CPC through a multimodal inhibitory mechanism [53]. The fact that the CPC molecules adhere to the steel surface implies that, depending on their concentration, they self-aggregate there to form a variety of stripes that are uniformly wide, regularly spaced, and well-organized. [54]. The surface is adequately covered by the molecules' long-range interactions, which lowers the rate of corrosion. On the surface of the steel, the CPC molecules are flat. When the pyridinium groups and side chains are near the steel surface, the ideal energy conditions are reached. [14].

The inertial axis of the molecule runs nearly parallel to the surface. This configuration of CPC molecules explains the high levels of IE on mild steel.

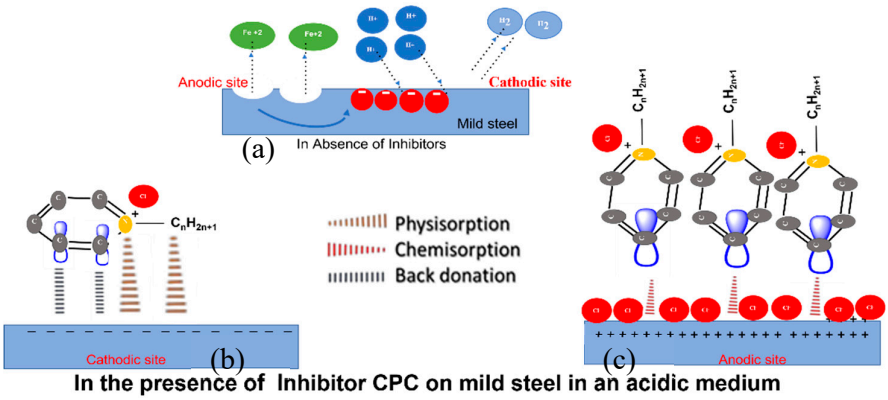

Figure 9.): Mechanism of CPC – Mild steel.

To predict the inhibition's adsorption mechanism onto the metal's surface, one must comprehend the corrosion mechanism of the metal [41]. This article describes the mechanism of mild steel corrosion in a solution of sulfuric acid.

The anodic dissolving mechanism of metals is the capacity of the free electron pairs on N and O to form a coordination with Fe shown in Figure 9b. Furthermore, the molecule's double bonds enable the interaction of metal d-electrons being donated in reverse to the p*-orbitals, which isn't feasible, for instance, with pyridinium. Furthermore, the p-electrons of the aromatic rings may interact with the metal surface [55]. Furthermore, after the basic functions of the inhibitor are protonated, electrostatic contact between the negatively charged iron surface (which may be caused by particular adsorption of Cl-anions) and the positively charged inhibitor is feasible, especially in acidic environments shown in Figure 9c. Essentially, the same interactions can happen in the case of a CPC inhibitor; the only difference is that neither nitrogen nor oxygen atoms are present. Because of their capacity to form metallic complexes, heat of hydrogenation, molecular size, the presence of free electron pairs in the N atoms, and the p-electrons on the aromatic rings, these compounds primarily prevent corrosion [56]. It is well known that ligands with the letters N have a coordination affinity towards mild steel. Thus, the adsorption on mild steel is caused by coordination between the p-electrons and heteroatoms of aromatic rings shown in Figure 9c. [23]. Pyridinium under study has the potential to form a bond with mild steel due to unshared electron pairs on N. The double bonds in the molecule also allow for back donation. The high inhibitory efficiency in CPC is caused by the presence of another hetero-atom N, which has a large number of free lone pairs of electrons that can interact with steel. It is well known that CPC produces a thin polymeric layer with excellent inhibitory efficacy on mild steel like Figure 9c [46].

In the instance of CPC, an extra anchoring point for the inhibitor to bond with the metal surface is provided by the lone pair of electrons of the pyridinium group's "N" atom connected to the pyridinium ring. This increases the strength of adsorption and, consequently, the inhibition.

 doi:10.20944/preprints202404.1187.v1

4. Conclusions

Based on the results and discussion, we concluded that CPC demonstrated good mild steel corrosion inhibitor performance in 0.5 M H2SO4, which is further strengthened in the presence of surfactants. CPC It implies that surfactants have an adsorption-based mechanism that affects the corrosion prevention activity of CPC. At every concentration under investigation, the weight loss measurement data point to an adsorption process that inhibits corrosion. FTIR measurement provides a comprehensive understanding of CPC adsorption on mild steel. As a combination inhibitor, CPC works. Research using FESM and AFM further supports the inhibitory nature of CPC. The high-resolution AFM micrographs showed that the corrosion of mild steel in 0.5 M H2SO4, solution was described by corrosion attack and the addition of inhibitor to the aggressive solutions diminished the corrosion of mild steel.

Author Contributions: Chandradip Kumar Yadav: Conceptualization, Data curation, Investigation, Writing-original draft. Amar Prasad Yadav, Shova Neupane, Benadict Rakesh: Methodology, Project administration. Tulasi Prasad Niraula, Ajaya Bhattarai: Formal analysis, Resources, Software, Funding acquisition, Validation, Visualization, Writing-review & editing.

Declaration of Competing Interest: The authors declare that they have no known competing financial interests or personal relationships that could have appeared to influence the work reported in this paper.

Funding: This research was funded by the University Grants Commission, Sanothimi, Bhaktapur, Nepal as partial grants for PhD under award No: 078/079, S&T-07 and INSA/DST/ISRF/2023/NEP/03.

Data Availability Statement: Suggested Data Availability Statements are available in the section "MDPI Research Data Policies" at https://www.mdpi.com/ethics.

Conflicts of Interest: The authors declare no conflicts of interest.

References

1. Alamry KA, Khan A, Aslam J, Hussein MA, Aslam R. Corrosion inhibition of mild steel in hydrochloric acid solution by the expired Ampicillin drug. Sci Rep [Internet]. 2023;13(1):1–15. Available from: https://doi.org/10.1038/s41598-023-33519-y
2. Tobsin T, Bangchit P, Sirikullertrat V, Sutthiruangwong S. Influence of Sodium Dodecyl Sulfate on Corrosion Behavior of 304 Stainless Steel. Thammasat Int J Sc Tech. 2010;15(3):40–6. https://ph02.tci-thaijo.org/index.php/SciTechAsia/article/view/41284
3. Nahlé A, Salim R, EL Hajjaji F, Ech-chihbi E, Titi A, Messali M, et al. Experimental and theoretical approach for novel imidazolium ionic liquids as Smart Corrosion inhibitors for mild steel in 1.0 M hydrochloric acid. Arab J Chem. 2022;15(8). https:// doi: 10.1016/j.arabjc.2022.103967.
4. Karki N, Neupane S, Gupta DK, Das AK, Singh S, Koju GM, et al. Berberine isolated from Mahonia nepalensis as an eco-friendly and thermally stable corrosion inhibitor for mild steel in acid medium. Arab J Chem [Internet]. 2021;14(12):103423. Available from: https://doi.org/10.1016/j.arabjc.2021.103423
5. Jafari H, Akbarzade K, Danaee I. Corrosion inhibition of carbon steel immersed in a 1 M HCl solution using benzothiazole derivatives. Arab J Chem [Internet]. 2019;12(7):1387–94. Available from: https://doi.org/10.1016/j.arabjc.2014.11.018
6. Arun A, Rajkumar K, Sasidharan S, Balasubramaniyan C. Process parameters optimization in machining of monel 400 alloy using abrasive water jet machining. Mater Today Proc [Internet]. 2023;98(August 2023):28–32. Available from: https://doi.org/10.1016/j.matpr.2023.08.308
7. Singh A, Singh VK, Quraishi MA. Aqueous extract of kalmegh (andrographis paniculata) leaves as green inhibitor for mild steel in hydrochloric acid solution. Int J Corros. 2010;2010. https://doi: 10.1155/2010/275983.
8. Elkacimi Y, Achnin M, Aouine Y, Touhami ME, Alami A, Touir R, et al. Inhibition of mild steel corrosion by some phenyltetrazole substituted compounds in hydrochloric acid. Port Electrochim Acta. 2011;30(1):53–65. https:// doi: 10.4152/pea.201201053.
9. Malik MA, Hashim MA, Nabi F, AL-Thabaiti SA, Khan Z. Anti-corrosion ability of surfactants: A review. Int J Electrochem Sci. 2011;6(6):1927–48. https://doi.org/10.1016/S1452-3981(23)18157-0
10. Bae K, Kang M, Shin Y, Choi E, Kim Y. Multifunctional Edible Oil-Impregnated Nanoporous Oxide Layer on AISI 304 Stainless Steel. 2023; https://doi.org/10.3390/nano13050807
11. Du H, Wen J, Song G, Wu H. Corrosion Behavior of Ni / NiCr / NiCrAlSi Composite Coating on Copper for Application as a Heat Exchanger in Sea Water. 2023; https://doi.org/10.3390/nano13243129

12. Park K, Chang BY, Hwang S. Correlation between Tafel Analysis and Electrochemical Impedance Spectroscopy by Prediction of Amperometric Response from EIS. ACS Omega. 2019;4(21):19307–13. https://doi.org/10.1021/acsomega.9b02672
13. Hamid ZA, Soror TY, El-Dahan HA, Omar AMA. New cationic surfactant as corrosion inhibitor for mild steel in hydrochloric acid solutions. Anti-Corrosion Methods Mater. 1998;45(5):306–11. https://doi.org/10.1108/00035599810234605
14. Fateh A, Aliofkhazraei M, Rezvanian AR. Review of corrosive environments for copper and its corrosion inhibitors. Arab J Chem [Internet]. 2020;13(1):481–544. Available from: https://doi.org/10.1016/j.arabjc.2017.05.021
15. Migahed MA, Al-Sabagh AM. Beneficial role of surfactants as corrosion inhibitors in petroleum industry: A review article. Chem Eng Commun. 2009;196(9):1054–75. https://doi.org/10.1080/00986440902897095
16. Gupta DK, Awasthi L, Das AK, Yadav B, Ghimire A, Yadav AP. Corrosion Inhibition Effect of Acidic Extract of Bark of Eucalyptus Globulus on Mild Steel. Tribhuvan Univ J. 2020;35(1):1–10. https://doi.org/10.3126/tuj.v35i1.35828
17. Mobin M, Parveen M, Rafiquee MZA. Synergistic effect of sodium dodecyl sulfate and cetyltrimethyl ammonium bromide on the corrosion inhibition behavior of L-methionine on mild steel in acidic medium. Arab J Chem. 2017;10(July):S1364–72. https://doi.org/10.1016/j.arabjc.2013.04.006
18. Bammou L, Belkhaouda M, Salghi R, Benali O, Zarrouk A, Zarrok H, et al. Corrosion inhibition of steel in sulfuric acidic solution by the Chenopodium Ambrosioides extracts. J Assoc Arab Univ Basic Appl Sci [Internet]. 2014;16:83–90. Available from: http://dx.doi.org/10.1016/j.jaubas.2013.11.001
19. Karki N, Neupane S, Chaudhary Y, Gupta DK, Yadav AP. Berberis aristata: A highly efficient and thermally stable green corrosion inhibitor for mild steel in acidic medium. Anal Bioanal Electrochem. 2020;12(7):970–88.
20. Bashir S, Singh G. Shatavari (Asparagus Racemosus) as Green Corrosion Inhibitor of Aluminium in Acidic Medium. 2019;37(2):83–91. doi: 10.4152/pea.201902083.
21. Gorker L, Dimitrov V. Modified tafel equation for electroless metal deposition. Prog React Kinet Mech. 2009;34(2):127–40.
22. Yıldız R, Arslanhan S, Döner A, Baran MF. Corrosion behavior of mild steel in 1 M HCl with Cyclotrichium niveum as a green inhibitor. Mater Chem Phys. 2024;312(November 2023):1–17. doi: 10.1016/j.matchemphys.2023.128654. doi: 10.1108/PRT-03-2018-0020.
23. Tucker IM, Burley A, Petkova RE, Hosking SL, Thomas RK, Penfold J, et al. Surfactant/biosurfactant mixing: Adsorption of saponin/nonionic surfactant mixtures at the air-water interface. J Colloid Interface Sci. 2020;574:385–92.
24. Ikeuba A. Green corrosion protection for mild steel in acidic media : saponins and crude extracts of Gongronema latifolium Pigment & Resin Technology Article information : 2018;(August).
25. Khadke P, Tichter T, Boettcher T, Muench F, Ensinger W, Roth C. A simple and effective method for the accurate extraction of kinetic parameters using differential Tafel plots. Sci Rep [Internet]. 2021;11(1):8974. Available from: https://doi.org/10.1038/s41598-021-87951-z
26. Yuningsih CR, Trihanondo D, Kusnadi J, Utami AK. Corrosion Inhibition Efficiency of Tamarindus Indica Leaves Extracts on Mild Steel in Hydrochloric Acid Corrosion Inhibition Efficiency of Terminalia Catappa Leaves Extracts on Stainless Steel in Hydrochloric Acid. https://doi: 10.1088/1742-6596/1378/2/022051.
27. Y. Musa A, H. kadhum AA, Takriff MS, Daud AR, Kamarudin SK. Investigation on Ethylenediaminetetra-Acetic Acid as Corrosion Inhibitor for Mild Steel in 1.0M Hydrochloric Acid. Mod Appl Sci. 2009;3(4). https:// doi: 10.5539/mas.v3n4p90.
28. Arrousse N, Fernine Y, Al-Zaqri N, Boshaala A, Ech-Chihbi E, Salim R, et al. Thiophene derivatives as corrosion inhibitors for 2024-T3 aluminum alloy in hydrochloric acid medium. RSC Adv. 2022;12(17):10321–35. https://doi: 10.1039/d2ra00185c.
29. Mirzaee E, Sartaj M. The application of surfactant-enhanced soil washing process combined with adsorption using a recoverable magnetic granular activated carbon for remediation of PAH-contaminated soil. Environ Adv [Internet]. 2022;9(April):100274. Available from: https://doi.org/10.1016/j.envadv.2022.100274
30. Oyewole O, Oshin TA, Atotuoma BO. Corchorus olitorius stem as corrosion inhibitor on mild steel in sulphuric acid. Heliyon [Internet]. 2021;7(4):e06840. Available from: https://doi.org/10.1016/j.heliyon.2021.e06840
31. Deef Allah M, Abdelhamed S, Soliman KA, El-Etre MA. The performance of three novel Gemini surfactants as inhibitors for acid steel corrosion: experimental and theoretical studies. RSC Adv. 2021;11(59):37482–97. https:// doi: 10.1039/d1ra07449k.
32. Gnanam S, Rajendran V. Influence of Various Surfactants on Size, Morphology, and Optical Properties of CeO 2 Nanostructures via Facile Hydrothermal Route . J Nanoparticles. 2013;2013:1–6.
33. Shahi N, Kumar S, Singh S, Kumar C, Yadav B, Prasad A, et al. International Journal of Electrochemical Science Comparison of dodecyl trimethyl ammonium bromide (DTAB) and cetylpyridinium chloride (

CPC) as corrosion inhibitors for mild steel in sulphuric acid solution. 2024;19(April). https://doi.org/10.1016/j.ijoes.2024.100575

34. Maiti K, Bhattacharya SC, Moulik SP, Panda AK. Physicochemistry of the binary interacting mixtures of cetylpyridinium chloride (CPC) and sodium dodecylsulfate (SDS) with special reference to the catanionic ion-pair (coacervate) behavior. Colloids Surfaces A Physicochem Eng Asp. 2010;355(1–3):88–98. https:// doi: 10.1016/j.colsurfa.2009.11.039.
35. Sethuraman MG, Raja PB. Corrosion inhibition of mild steel by Datura metel in acidic medium. Pigment Resin Technol. 2005;34(6):327–31. https:// doi: 10.1108/03699420510630345.
36. Mauro AC, Ribeiro BD, Garrett R, Borges RM, Da Silva TU, Paula Machado S De, et al. Ziziphus joazeiro stem bark extract as a green corrosion inhibitor for mild steel in acid medium. Processes. 2021;9(8):1–22. http:// doi: 10.3390/pr9081323..
37. Wang M, Du H, Guo A, Hao R, Hou Z. Microstructure control in ceramic foams via mixed cationic/anionic surfactant. Mater Lett [Internet]. 2012;88:97–100. Available from: http://dx.doi.org/10.1016/j.matlet.2012.08.028
38. Jia H, Lian P, Leng X, Han Y, Wang Q, Jia K, et al. Mechanism studies on the application of the mixed cationic/anionic surfactant systems to enhance oil recovery. Fuel [Internet]. 2019;258(August):116156. Available from: https://doi.org/10.1016/j.fuel.2019.116156
39. Goldraich M, Schwartz JR, Burns JL, Talmon Y. Microstructures formed in a mixed system of a cationic polymer and an anionic surfactant. Colloids Surfaces A Physicochem Eng Asp. 1997;125(2–3):231–44. http://doi: 10.1016/S0927-7757(96)03895-2.
40. Fayomi OSI, Popoola API, Oloruntoba T, Ayoola AA. Inhibitive characteristics of cetylpyridinium chloride and potassium chromate addition on type A513 mild steel in acid/chloride media. Cogent Eng. 2017;4(1):1–9. http://doi: 10.1080/23311916.2017.1318736.
41. Nallakukkala S. Comparative Study of Corrosion Inhibition in Carbon Steel Using Non-ionic Surfactants in Acidic Medium. Int J Chem Eng Process [Internet]. 2018;4(January):1. Available from: www.journalspub.com
42. Anderson AR. The Characteristics Of A True Leader. 2013;(January 2005). Available from: http://www.forbes.com/sites/amyanderson/2015/03/01/the-characteristics-of-a-true-leader/#470b00825bf7
43. Holland PM, Rubingh DN. Mixed Surfactant Systems. Fuel Sci Technol Int. 1993;11(1):241–2. http://doi: 10.1080/08843759308916065.
44. Ramezanzadeh M, Sanaei Z, Bahlakeh G, Ramezanzadeh B. Highly effective inhibition of mild steel corrosion in 3.5% NaCl solution by green Nettle leaves extract and synergistic effect of eco-friendly cerium nitrate additive: Experimental, MD simulation and QM investigations [Internet]. Vol. 256, Journal of Molecular Liquids. Elsevier B.V; 2018. 67–83 p. Available from: https://doi.org/10.1016/j.molliq.2018.02.021
45. Pon-On W, Meejoo S, Tang IM. Formation of hydroxyapatite crystallites using organic template of polyvinyl alcohol (PVA) and sodium dodecyl sulfate (SDS). Mater Chem Phys. 2008;112(2):453–60. http:// doi: 10.1016/j.matchemphys.2008.05.082. doi: 10.3126/jncs.v44i1.62690.
46. Yadav CK, Niraula TP, Neupane S, Yadav AP, Bhattarai A. Study of Anti-Corrosion Properties of Sodium Dodecyl Sulphate and Cetyl Pyridinium Chloride. J Nepal Chem Soc. 2024;44(1):163–72. http://doi: 10.3126/jncs.v44i1.62690.
47. Lone MS, Afzal S, Chat OA, Aswal VK, Dar AA. Temperature-and composition-induced multiarchitectural transitions in the catanionic system of a conventional surfactant and a surface-active ionic liquid. ACS Omega. 2021;6(18):11974–87. http://doi: 10.1021/acsomega.1c00469.
48. Ghosh D, Bhattarai A, Das B. Electrical conductivity of sodium polystyrenesulfonate in acetonitrile - Water-mixed solvent media: Experiment and data analysis using the Manning counterion condensation model and the scaling theory approach. Colloid Polym Sci. 2009 Sep;287(9):1005–11. doi: 10.1007/s00396-009-2055-7.
49. Chemistry P. Micellar Characterisation of Saponin from Sapindus Mukorossi. 2006;43:262–8. https://doi.org/10.3139/113.100315
50. Ramírez Coutiño VA, Torres Bustillos LG, Godínez Mora Tovar LA, Guerra Sánchez RJ, Rodríguez Valadez FJ. pH effect on surfactant properties and supramolecular structure of humic substances obtained from sewage sludge composting. Rev Int Contam Ambient. 2013;29(3):191–9.
51. Sachin KM, Karpe S, Singh M, Bhattarai A. Physicochemical Properties of Dodecyltrimethylammonium Bromide (DTAB) and SodiumDodecyl Sulphate (SDS) Rich Surfactants in Aqueous Medium, At T = 293.15, 298.15, and 303.15 K. Macromol Symp. 2018 Jun 1;379(1). http:// doi: 10.1002/masy.201700034.
52. Belhaj AF, Elraies KA, Mahmood SM, Zulkifli NN, Akbari S, Hussien OSE. The effect of surfactant concentration, salinity, temperature, and pH on surfactant adsorption for chemical enhanced oil recovery: a review. J Pet Explor Prod Technol [Internet]. 2020;10(1):125–37. Available from: https://doi.org/10.1007/s13202-019-0685-y
53. Mondal BB, Banik R, Ghosh S. n Pr f. Colloids Surfaces A Physicochem Eng Asp [Internet]. 2023;132781. Available from: https://doi.org/10.1016/j.colsurfa.2023.132781

 doi:10.20944/preprints202404.1187.v1

54. Kupsch S, Eggers LF, Spengler D, Gisch N, Goldmann T, Fehrenbach H, et al. Characterization of phospholipid-modified lung surfactant in vitro and in a neonatal ARDS model reveals anti-inflammatory potential and surfactant lipidome signatures. Eur J Pharm Sci [Internet]. 2022;175(December 2021):106216. Available from: https://doi.org/10.1016/j.ejps.2022.106216
55. Abdallah M, Soliman KA, Al-Gorair AS, Al Bahir A, Al-Fahemi JH, Motawea MS, et al. Enhancing the inhibition and adsorption performance of SABIC iron corrosion in sulfuric acid by expired vitamins. Experimental and computational approach. RSC Adv. 2021;11(28):17092–107. http://doi: 10.1039/d1ra01010g.
56. Pavelyev RS, Zaripova YF, Yarkovoi V V., Vinogradova SS, Razhabov S, Khayarov KR, et al. Performance of waterborne polyurethanes in inhibition of gas hydrate formation and corrosion: Influence of hydrophobic fragments. Molecules. 2020;25(23). http://doi: 10.3390/molecules25235664.